Title
Mass Spectral Profiling of Glycosaminoglycans from Histological Tissue Surfaces

Journal
Analytical Chemistry, 85(22)

ISSN
0003-2700

Authors
Shao, Chun
Shi, Xiaofeng
Phillips, Joanna J
et al.

Publication Date
2013-11-19

DOI
10.1021/ac402517s

Peer reviewed

Published in final edited form as:
Anal Chem. 2013 November 19; 85(22): . doi:10.1021/ac402517s.

Mass spectral profiling of glycosaminoglycans from histological tissue surfaces

Chun Shao[1], **Xiaofeng Shi**[1], **Joanna J. Phillips**[2], and **Joseph Zaia**[1]

[1]Center for Biomedical Mass Spectrometry, Department of Biochemistry, Boston University School of Medicine

[2]Department of Neurological Surgery, Division of Neuropathology, Department of Pathology University of California, San Francisco.

Abstract

Glycosaminoglycans (GAGs) are found in intracellular granules, cell surfaces and extracellular matrices in a spatially and temporally regulated fashion, constituting the environment for cells to interact, migrate and proliferate. Through binding with a great number of proteins, GAGs regulate many facets of biological processes from embryonic development to normal physiological functions. GAGs have been shown to be involved in pathologic changes and immunological responses including cancer metastasis and inflammation. Past analyses of GAGs have focused on cell lines, body fluids and relatively large tissue samples. Structures determined from such samples reflect the heterogeneity of the cell types present. In order to gain an understanding of the roles played by GAG expression during pathogenesis, it is very important to be able to detect and profile GAGs at the histological scale so as to minimize cell heterogeneity to potentially inform diagnosis and prognosis.

Heparan sulfate (HS) belongs to one major class of GAGs, characterized by dramatic structural heterogeneity and complexity. In order to demonstrate feasibility of analysis of HS, 13 μm frozen bovine brain stem, cortex and cerebellum tissue sections were washed with a series of solvent solutions to remove lipids before applying heparin lyases I, II, and III on the tissue surfaces within 5mm*5mm digestion spots. The digested HS disaccharides were extracted from tissue surfaces and then analyzed by using size exclusion chromatography/mass spectrometry (SEC-MS). The results from bovine brain stem, cortex and cerebellum demonstrated the reproducibility and reliability of our profiling method. We applied our method to detect HS from human astrocytoma (WHO grade II) and glioblastoma (GBM, WHO grade IV) frozen slides. Higher HS abundances and lower average sulfation level of HS were detected in glioblastomas (GBM, WHO grade IV) slides compared to astrocytoma WHO grade II slides.

Introduction

Glycosaminoglycans (GAGs) are a family of linear sulfated polysaccharides found in cellular granules on cell surfaces and in extracellular matrices of animal cells. Among GAGs, heparin, heparan sulfate (HS), chondroitin sulfate (CS), and dermatan sulfate (DS) bind many families of growth factors and growth factor receptors[1, 2]. They serve as co-receptors for growth factor-growth factor receptor interactions and bind growth factors and other proteins in the extracellular matrix. Such GAG-protein interactions are necessary for embryogenesis and the functioning of every adult physiological system[3]. GAG chains are

Address for correspondence: Joseph Zaia Boston University Medical Campus 670 Albany St., Boston, MA 02118 (v) 617-638-6762 (e) jzaia@bu.edu.

heterogeneous, and their structures vary according to tissue type[4]. While there is general appreciation regarding the regulated nature of GAG chain structure, it has not been possible to produce sufficient structural information to understand their roles in disease states including cancers.

GAGs are expressed in a spatially and temporally regulated manner[5]. Thus, the structure and abundance of GAG chains varies according to the cell type, developmental state, and regulatory signals received from the extracellular matrix. Understanding of the roles of GAGs in physiology therefore depends on the ability to determine the structures and abundances of GAGs from small quantities of tissue.

We and others have studied the expression of GAGs in tissue related to a variety of disease states[6-14]. These studies leveraged the ability to extract GAGs from comparatively small quantities of tissue[15, 16]. Thus, it was possible to compare structures of chondroitin/dermatan sulfate in human squamous cell carcinoma biopsies[6]. It was clear from these studies, however, that the heterogeneity of the biopsy tissue limited the ability to determine the structures of GAGs expressed by cancer cells versus those from surrounding non-cancerous cells. We therefore sought to develop methods to analyze GAGs from smaller tissue quantities.

MALDI-based imaging mass spectrometry (IMS) has advanced to the point that protein and lipid profiles can be obtained on tissue spots less than 25 microns[17]. Glycoconjugate glycans, however, are not typically observed in MALDI IMS experiments. Glycans dissociate under typical vacuum MALDI conditions, a fact that is likely to limit the ability to perform tissue-based imaging and profiling experiments. In addition, ionization of glycans, as hydrophilic molecules, is easily suppressed by more hydrophobic proteins and lipids present in the tissue. The analysis of *N*-glycans enzymatically released from tissue surfaces has been accomplished by permethylation prior to MALDI-TOF mass spectrometry[18]. These results demonstrate the validity of derivatization to improve the stability and ionization responses of the *N*-glycans. In order to analyze GAGs as permethylated derivatives, it is necessary to use a multistep derivatization process in which sulfate groups are replaced by acetate groups prior to MS analysis[19]. We have chosen to analyze GAGs enzymatically released from tissue surfaces in native form in order to keep the analytical workflow as simple as possible.

Analysis of GAGs from tissue sections was first reported for hyaluronan and chondroitin sulfate and was carried out using formalin fixed paraffin embedded tissue that had been subsequently de-waxed and re-hydrated before applying GAG-degrading enzymes[20, 21]. The released GAG disaccharides were then detected using reversed phase ion pairing chromatography with post-column fluorescence derivatization and detection. Tissue may also be embedded in optimal cutting temperature polymer, sectioned using a cryostat, fixed with methanol and dried on a glass slide. Chondroitin/dermatan sulfate GAGs have been analyzed from tumor tissue prepared in this way on glass slides by adding enzyme digestion solution to the dried tissue. The digest was analyzed by reversed phase ion pairing LC/MS[22]. Corneal keratin sulfate (KS) GAGs were analyzed from fresh frozen tissue sections by applying a ring around tissue to be analyzed using a hydrophobic pen[23, 24] followed by direct electrospray mass spectrometric analysis of mono- and di-sulfated disaccharide products.

Given the feasibility of ESI mass spectral analysis of GAGs from tissue surfaces, we sought to develop methods appropriate for quantitative studies. A reproducible and quantitative method is necessary in order to compare the structures of GAGs expressed in normal versus disease tissue. We were concerned that surface effects would limit the reproducibility of

direct MS analysis of enzyme digest solutions. Size exclusion chromatography (SEC)-MS has proven to be extremely useful for quantitative comparison of GAG disaccharide profiles among tissue and cell types[6, 15, 25-31]. The method is very robust and removes components from the tissue that interfere with ionization of the disaccharide analytes. Therefore, we compared direct nano-ESI *versus* SEC-MS methods of quantification of GAGs released from tissue surfaces. The results demonstrated that both CS/DS and HS GAGs may be analyzed reproducibly from slides prepared from frozen tissue. The method was applied to analysis of HS from human glioma biopsies.

Experimental section

Materials

Frozen bovine cortex, brain stem and cerebellum slides, which were cut at a thickness of 15 μm, and the tissue blocks from which the slides were prepared were purchased from Zyagen (San Diego, CA). Each slide contained two sections. Frozen diffuse astrocytoma (WHO grade II) slides and glioblastoma (GBM, WHO grade IV) slides, which were cut at a thickness of 10 μm, were prepared at University of California San Francisco. Each slide contains one section. Heparin lyase I was purchased from New England Biolabs (Andover, MA) and heparin lyases II and III were generous gifts from Prof. Jian Liu (UNC Eshelman School of Pharmacy, USA). Heparan sulfate sodium salt from porcine intestinal mucosa (HSPIM) was purchased from Celsus Laboratories (Cincinnati, OH).

Fresh tissue slides processing before enzymatic digestion

Frozen tissue slides were washed using chloroform:methanol solution (v/v=7:3) for 10 min, twice, to remove lipids. Isopropanol:distilled water solution (v/v=1:1) was then used to wash the slides for 10 min, twice. A 20 mM ammonium bicarbonate solution (pH adjusted to 9.0) was applied to dissolve acidic molecules on the tissue surfaces for 10 min, twice. The tissue slides were then washed using distilled water for 10 min, three times. The slides were then allowed to dry in air.

Enzyme digestions for HS at tissue surfaces

Three digestion spots (with the size of 5mm × 5mm) were chosen in each frozen bovine cortex, brain stem and cerebellum frozen histological section. Ten serial sections were used for each sample to verify the reproducibility of the method and the spatial positions of digestion spots were carefully coordinated.

Fresh frozen histological slides were prepared for three diffuse astrocytomas biopsies samples and five GBM biopsies samples were prepared. One or two digestion spots were chosen from each frozen section. The number of digestion spots was determined by the histological characteristics of the sample. Three serial sections were used for each sample and the spatial positions of the digestion spots were also carefully coordinated. The abundances of disaccharides were normalized to $1mm^2$ digestion spot size.

The tissue slides were put in a sealed box during digestion to maintain an atmosphere saturated with water vapor at 37 °C. A 5 μl volume of enzyme solution I, containing 20 mU of heparin lyase I (specific for highly sulfated HS domains), 2 mU of heparin lyase III (specific for HS domains with a low degree of sulfation) and 2 mU of heparin lyase II (cleaves all HS domains) in the presence of 10 mM Tris/HCl buffer pH7.4 and 2 mM $CaCl_2$, was added to the defined digestion spot at 37 °C for 45 min. In order to keep the digestion spot wet, a 5 μl volume distilled water was then added and the digestion was allowed to proceed for another 45 min at 37 °C. The cycle of addition of enzyme solution I and distilled water was then repeated 3 more times. Finally, 5 μl enzyme solution II containing only 20

mU of heparin lyase I, 2 mU of heparin lyase II and 2 mU of heparin lyase III was added for 45 min at 37 °C. The digested products were aspirated by pipetting 6 μl 0.3% ammonium hydroxide solution into each digestion spots. Aspiration steps were repeated for another 5 times and the extraction volumes were combined. The solutions extracted from each spot were dried using a vacuum concentrator and dissolved in 10 μl distilled water.

The methods for GAG extraction from tissue blocks, enzyme digestion of HS from tissue blocks, SEC-MS, and direct nano-ESI MS are given in the Supplemental Methods section. The SEC-MS method and appearance of GAG disaccharide mass spectra produced has been described previously[15].

Results

SEC-MS is a reliable and robust method to analyze HS released from tissue surfaces

Heparan sulfate can be digested into disaccharides using heparin lyases I, II, and III. The structures of HS disaccharides are designated using the coding system of *Lawrence et al*[32], summarized in Scheme S-1. Among unsaturated disaccharides, D0A0, D0S0, D0A6/D2A0 and D0S6/D2S0 are the four most abundant signals detected from typical HS sources. HS disaccharides extracted from two spots in the bovine hippocampus, cortex, cerebellum and brain stem slides were analyzed by both direct nano-ESI MS and SEC-MS, as shown in Figure S1. Despite the convenience, direct nano-ESI MS produced considerably higher variability between the paired spots for each brain tissue than did SEC-MS. We concluded that molecules co-extracted from the tissue surfaces influenced the abundances of ions detected using direct nano-ESI MS. The use of SEC-MS appears to remove tissue surface molecules that interfere with direct nano-ESI MS analysis and was used for the remainder of the experiments here described. Representative SEC-MS total ion chromatograms (TICs) and extracted ion chromatograms (EICs) for HS unsaturated disaccharides acquired from frozen bovine brain stem and human GBM slides are shown in Figure 1.

Recovery of HS disaccharides from tissue surfaces

In order to determine the efficiency of recovery of HS from the tissue surfaces, we digested HS from tissue surfaces using heparin lyases and extracted the disaccharides. We then verified that no additional disaccharides could be extracted after additional digestion using lyases. Next, we deposited 0.75 μg HSPIM onto the tissue surfaces where HS had been digested and extracted previously and used the same conditions described in the experimental procedures to exhaustively digest 0.75 μg HSPIM. Figure 2 compares the absolute (A) and relative (B) abundances for five unsaturated HS disaccharides digested in solution versus on the frozen bovine cortex tissue slides. The coefficients of variation (CV) for the absolute and relative abundances from three independent experiments were less than 5% for all disaccharides except for the lowest in abundance (D2A6), indicating extraction step is consistent among different spots. The recovery for each digested HS disaccharide from tissue surfaces was about 90%, as shown in Figure 2A. In addition, the differences of the relative abundance for the five most abundant disaccharides were 1.3% or less, as shown in Figure 2B. Digestion of 0.75 ug HSPIM produces approximately 50 times more disaccharides than typically present on the surfaces of tissue slides. Therefore, the enzymatic digestion protocol is more than sufficient to digest all HS present on histological slides. We also deposited 2.5, 5, and 10 pmol of HS disaccharide standards, respectively, onto different tissue spots. These quantities approximate those typically found on histological slide surfaces. Figure S-2 shows that the extraction efficiencies for HS disaccharides standards are over 90%, confirming the reliability of extraction step. In summary, the recovery of digested disaccharides and disaccharides standards from tissue surface is acceptable and consistent among different spots.

Method reproducibility and spatial variability for bovine brain stem, cortex and cerebellum

We conducted the following experiment to demonstrate that instrument sensitivity was appropriate for analysis of HS from fresh frozen tissue slides. As shown in the Figure S-3, 2.5 pmol HS standards containing D0A0, D0S0, D0A6, D0S6, D2A6 and D2S6 gave acceptable EIC peaks. The signal to noise ratio (S/N) for each disaccharide monoisotopic peak was 6 or greater and the coefficient of variation less than 6%. Because the abundances of D0A0, D0S0 and D0S6/D2S0 ions observed from bovine brain, human astrocytomas and GBM slides correspond to greater than 2.5 pmol and that for D0A6/D2A0 to 2 pmol, we concluded that the instrument sensitivity was adequate.

In order to demonstrate the reproducibility of our method, we used 10 serial frozen sections from brain stem, cortex and cerebellum from a single bovine brain. A set of three spots was selected for each tissue section, the position of which was reproduced in each serial section. The absolute and relative HS disaccharide abundances released from bovine brain stem slides are shown in Figure 3A and 3B. Statistical analysis of variance (ANOVA) tests were applied to demonstrate the reproducibility with respect to the three spots on each tissue slide. As shown in Figure 3B, p values for disaccharide relative abundances greater than 5% were not significant among the three spots. With regard to the relative abundances, CV values for D0A0 and D0S0 are approximately 5% and those for D0A6/D2A0 and D0S6/D2S0 approximately 12%. We therefore concluded that HS disaccharide composition was relatively homogenous in bovine brain stem. The CV values for the absolute abundances of D0A0, D0S0, D0A6/D2A0, and D0S6/D2S0 from ten serial sections were approximately 15% for each of the three spots. Since the CV value for the recovery of HSPIM standards is around 5%, the observed 15% CV for ten serial sections is not caused by variation in HS recovery from the tissue surfaces. This indicates that the CV value reflects variation in the amount of HS present in the series of bovine brain stem sections. These data also show that the HS quantity present among the three digestion spots varies significantly and is likely to due to spatial differences in tissue morphology. We then compared the abundances of disaccharides extracted from the tissue block from which slides were prepared versus digestion from tissue slides (Figure S-4). The relative disaccharides abundances showed a 3% difference between mean value of tissue block and tissue surface for D0A0 and D0S0, 1% for D0A6/D2A0 and 1.7% for D0S6/D2S0. This confirms the reliability of our method.

We observed similar results for the same experiment using slides from bovine cortex, as shown in Figure 4A and 4B. Statistical analysis of variance (ANOVA) of the data showed p values (shown in the figure) that indicated significant differences among three digestions spots in terms of the absolute disaccharides abundances. ANOVA calculations showed that the relative abundances had p values > 0.05, indicating that they were not significantly different. The CV values for the absolute abundances of D0A0, D0S0, D0A6/D2A0, and D0S6/D2S0 from ten serial sections were approximately 15%. The CV values for the relative abundances were D0A0 (5%), D0S0 (5%), D0A6/D2A0 (8%), and D0S6/D2S0 (12%). In summary, the slight differences among absolute disaccharide abundances among serial sections were also detected in bovine cortex, which is acceptable for biological samples. The data also demonstrated that statistically significant differences in HS absolute abundances were present among the three digestion spots on each tissue slide. In addition, a 2.5% difference between mean relative abundance values for tissue block *versus* tissue surface was observed for D0A0 and D0S0 and 0.5% for D0A6/D2A0 (Figure S-5).

As shown in Figure 5A, ANOVA calculations showed p values > 0.05, indicating no significant differences in absolute disaccharide abundances among three spots digested on bovine cerebellum tissue slides. These slides produced high CV values of approximately 40%. H&E staining was applied to see the morphological characteristics of cerebellum continuous slides (Figure S-6). These data show that variability of cerebellum tissue

morphology among serial sections, give rise to the observed high CV values. As with the other bovine brain tissues, p values for relative disaccharide abundances were > 0.05 for three spots (Figure 5B). The CV values for the relative disaccharide abundances of D0A0 and D0S0 were approximately 5%, and those for D0A6/D2A0 and D0S6/D2S0 approximately 10%. A 1% difference between mean value for disaccharides extracted from tissue block *versus* tissue surface was observed for D0A0 and 3% for D0S0 and D0A6/D2A0 (Figure S-7).

Application to human glioma samples

Astrocytomas and GBMs represent different stages of human gliomas. We applied our method to profile HS in 3 astrocytoma samples and 4 GBM samples. It is interesting to note that ANOVA calculations showed that absolute abundances for HS disaccharides were significantly higher in GBM than astrocytomas, as shown in Figure 6A. The CVs for the absolute disaccharide abundances were within 15% for each individual. In addition, ANOVA calculations showed that statistically significant increases in relative abundances of D0A0% and D0S0% and decreases in D0A6/D2A0% and D0S6/D2S0% in GBMs compared with astrocytomas, indicating lower sulfation level in GBMs. The CV values for the relative abundances of D0A0 and D0S0 were approximately 5% and those for D0A6/D2A0 and D0S6/D2S0 approximately 10% for each individual. We collected data demonstrating that the SEC-MS instrument was stable (with CV values for the absolute abundances of D0A0, D0S0, D0A6/D2A0, D0S6/D2S0 and D2A6 were less than 5%) over the duration of the time during which the data were acquired (Figure S-8). We therefore conclude that there are significant differences in HS disaccharide abundances between the set of GBM and astrocytoma samples analyzed in this work.

Discussion and conclusions

Profiling HS from histological tissue surfaces by SEC-MS provides a sensitive and feasible method to understand HS structure and distribution than traditional extraction HS from whole tissue and provides a means of limiting tissue heterogeneity. The traditional method for extraction of HS from wet tissue requires several days to complete and a minimum of 10 mg wet tissue weight. The on-slide digestion we show can be accomplished by digesting a tissue slide corresponding to a fraction of a milligram tissue with no prior extraction necessary.

There is increasing evidences showing involvement of proteoglycans in cancer development, metastasis and other pathogenic processes *in vivo and in vitro*. The majority of these studies focus on core protein expression levels due to lack of appropriate methods for the GAG chains. To better understand the roles of GAGs in cancer development, it is important to compare the GAG quantities and structures between tumor and normal tissue. Considering the heterogeneity of normal tissue and the tumor microenvironment, we developed a profiling method for GAG applicable to the histological scale. Our method is reproducible and sensitive enough for studies of human brain gliomas. The results have the potential to shed light on the role of GAG in pathogenic processes.

In summary, the results shown here demonstrate the feasibility of recovering GAGs from histological surfaces. GAG abundances differ according to location, indicating the importance of achieving reproducible analysis. We demonstrate that SEC-MS enables considerably more reproducible analysis than does direct ESI-MS of enzyme digestion solutions, presumably due to the removal of molecules that interfere with analyte ionization. SEC-MS is slow, however, indicating that more rapid LC-MS methods are needed. We recently published a HILIC-MS method for disaccharide analysis [33] and are in the process of optimizing it for rapid analysis of tissue GAGs at reduced chromatography scale.

Supplementary Material

Refer to Web version on PubMed Central for supplementary material.

Acknowledgments

This work was funded by NIH grants P41GM104603 and R01HL098950.

References

(1). Bernfield M, Gotte M, Park PW, Reizes O, Fitzgerald ML, Lincecum J, Zako M. Annu Rev Biochem. 1999; 68:729–777. [PubMed: 10872465]

(2). Sugahara K, Mikami T, Uyama T, Mizuguchi S, Nomura K, Kitagawa H. Curr Opin Struct Biol. 2003; 13:612–620. [PubMed: 14568617]

(3). Bishop JR, Schuksz M, Esko JD. Nature. 2007; 446:1030–1037. [PubMed: 17460664]

(4). Maccarana M, Sakura Y, Tawada A, Yoshida K, Lindahl U. J Biol Chem. 1996; 271:17804–17810. [PubMed: 8663266]

(5). Kreuger J, Spillmann D, Li JP, Lindahl U. The Journal of cell biology. 2006; 174:323–327. [PubMed: 16880267]

(6). Thelin M, Svensson KJ, Shi X, Bagher M, Axelsson J, Isinger-Ekstrand A, van Kuppevelt TH, Johansson J, Nilbert M, Zaia J, Belting M, Maccarana M, Malmstrom A. Cancer Res. 2012; 72:1943–1952. [PubMed: 22350411]

(7). Bielik AM, Zaia J. Methods Mol Biol. 2010; 600:215–225. [PubMed: 19882131]

(8). Hitchcock A, Yates KE, Costello C, Zaia J. Proteomics. 2008; 8:1384–1397. [PubMed: 18318007]

(9). Weyers A, Yang B, Yoon DS, Park JH, Zhang F, Lee KB, Linhardt RJ. Omics : a journal of integrative biology. 2012; 16:79–89. [PubMed: 22401653]

(10). Yoneda A, Lendorf ME, Couchman JR, Multhaupt HA. The journal of histochemistry and cytochemistry : official journal of the Histochemistry Society. 2012; 60:9–21. [PubMed: 22205677]

(11). Phillips JJ, Huillard E, Robinson AE, Ward A, Lum DH, Polley MY, Rosen SD, Rowitch DH, Werb Z. The Journal of clinical investigation. 2012; 122:911–922. [PubMed: 22293178]

(12). Vlodavsky I, Beckhove P, Lerner I, Pisano C, Meirovitz A, Ilan N, Elkin M. Cancer Microenviron. 2011

(13). Rosen SD, Lemjabbar-Alaoui H. Expert opinion on therapeutic targets. 2010; 14:935–949. [PubMed: 20629619]

(14). Sasisekharan R, Shriver Z, Venkataraman G, Narayanasami U. Nat Rev Cancer. 2002; 2:521–528. [PubMed: 12094238]

(15). Shi X, Zaia J. J Biol Chem. 2009; 284:11806–11814. [PubMed: 19244235]

(16). Guimond SE, Puvirajesinghe TM, Skidmore MA, Kalus I, Dierks T, Yates EA, Turnbull JE. J Biol Chem. 2009; 284:25714–25722. [PubMed: 19596853]

(17). Zavalin A, Todd EM, Rawhouser PD, Yang J, Norris JL, Caprioli RM. Journal of mass spectrometry : JMS. 2012; 47:1473–1481. [PubMed: 23147824]

(18). Hu Y, Zhou S, Khalil SI, Renteria CL, Mechref Y. Analytical chemistry. 2013; 85:4074–4079. [PubMed: 23438902]

(19). Huang R, Pomin VH, Sharp JS. Journal of the American Society for Mass Spectrometry. 2011; 22:1577–1587. [PubMed: 21953261]

(20). Koshiishi I, Horikoshi E, Imanari T. Anal Biochem. 1999; 267:222–226. [PubMed: 9918675]

(21). Koshiishi I, Takenouchi M, Imanari T. Archives of Biochemistry and Biophysics. 1999; 370:151. [PubMed: 10510272]

(22). Oguma T, Toyoda H, Toida T, Imanari T. Biomed Chromatogr. 2001; 15:356–362. [PubMed: 11507718]

(23). Conrad AH, Zhang Y, Walker AR, Olberding LA, Hanzlick A, Zimmer AJ, Morffi R, Conrad GW. Invest Ophthalmol Vis Sci. 2006; 47:120–132. [PubMed: 16384953]

(24). Zhang Y, Conrad AH, Tasheva ES, An K, Corpuz LM, Kariya Y, Suzuki K, Conrad GW. Investigative Ophthalmology and Visual Science. 2005; 46:1604–1614. [PubMed: 15851558]

(25). Tran TH, Shi X, Zaia J, Ai X. J Biol Chem. 2012; 287:32651–32664. [PubMed: 22865881]

(26). Shi X, Huang Y, Mao Y, Naimy H, Zaia J. J Am Soc Mass Spectrom. 2012; 23:1498–1511. [PubMed: 22825743]

(27). Schumacher VA, Schlotzer-Schrehardt U, Karumanchi SA, Shi X, Zaia J, Jeruschke S, Zhang D, Pavenstaedt H, Drenckhan A, Amann K, Ng C, Hartwig S, Ng KH, Ho J, Kreidberg JA, Taglienti M, Royer-Pokora B, Ai X. J Am Soc Nephrol. 2011; 22:1286–1296. [PubMed: 21719793]

(28). Langsdorf A, Schumacher V, Shi X, Tran T, Zaia J, Jain S, Taglienti M, Kreidberg JA, Fine A, Ai X. Glycobiology. 2011; 21:152–161. [PubMed: 20855470]

(29). Crouch E, Nikolaidis N, McCormack F, McDonald B, Allen K, Rynkiewicz M, Cafarella T, White M, Lewnard K, Leymarie N, Zaia J, Seaton B, Hartshorn K. J Biol Chem. 2011; 286:40681–40692. [PubMed: 21965658]

(30). Staples GO, Shi X, Zaia J. J Biol Chem. 2010; 285:18336–18343. [PubMed: 20363743]

(31). Hitchcock AM, Costello CE, Zaia J. Biochemistry. 2006; 45:2350–2361. [PubMed: 16475824]

(32). Lawrence R, Lu H, Rosenberg RD, Esko JD, Zhang L. Nat Methods. 2008; 5:291–292. [PubMed: 18376390]

(33). Gill VL, Aich U, Rao S, Pohl C, Zaia J. Analytical chemistry. 2013; 85:1138–1145. [PubMed: 23234263]

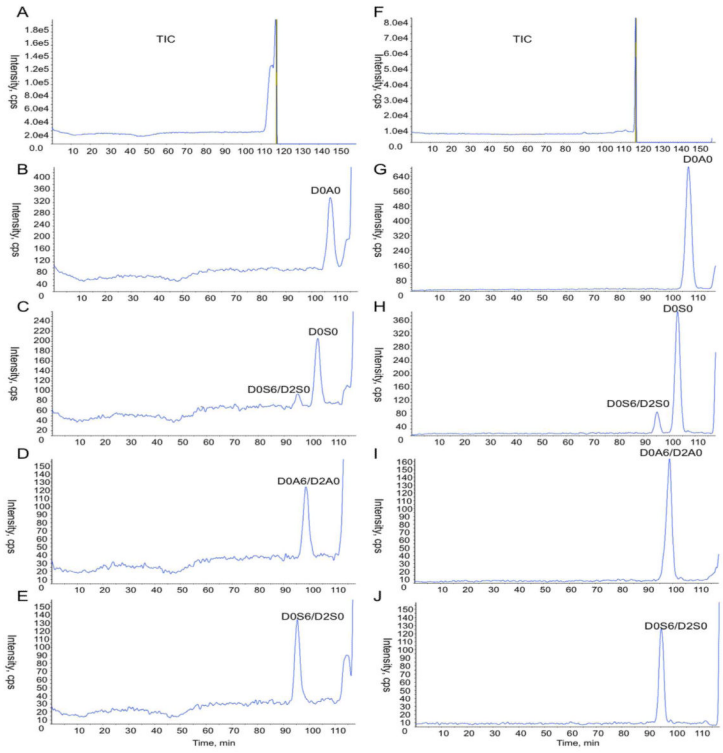

Figure 1.

Representative total ion chromatograms (TICs) and extracted ion chromatograms (EICs) for HS unsaturated disaccharides from fresh frozen histology slides: bovine brain stem (A-E) and human glioblastoma (F-J). The D2A6 and D2S6 disaccharides from tissue sections were not detected. Two peaks for D0S6/D2S0 were detected because of in-source loss of SO_3. The loss of SO_3 was corrected for the quantification as described[15].

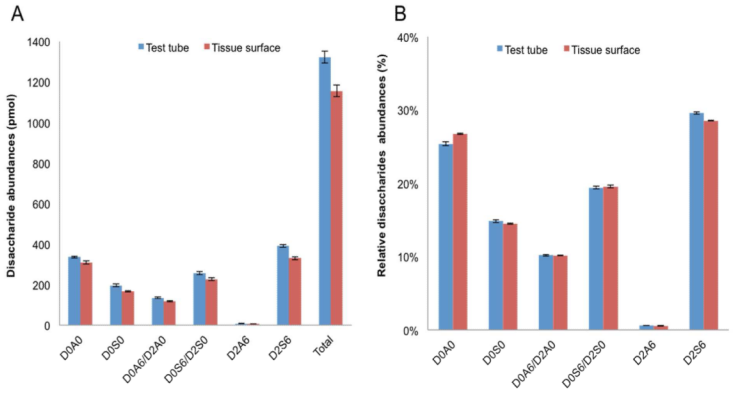

Figure 2.

Comparison of the recovery of HSPIM disaccharides digested on bovine brain stem tissue surface *versus* in solution. (A) Absolute disaccharides ion abundances; (B) relative disaccharides ion abundances. The height of each bar is the mean value of three independent experiments. The error bars represent the standard error.

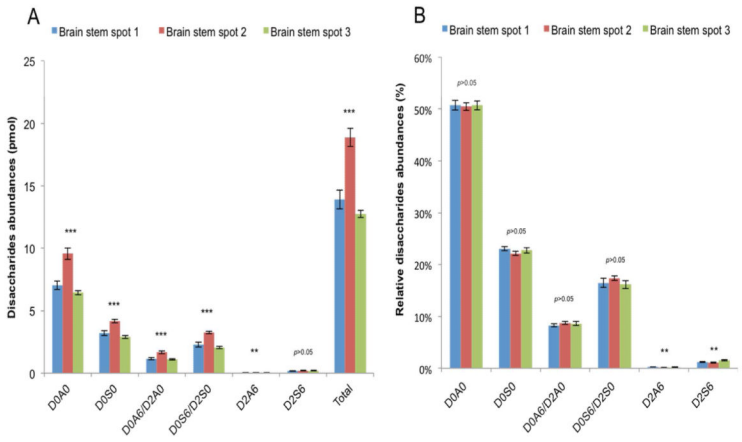

Figure 3.

Ion abundances of HS disaccharides from bovine brain stem tissue slides corresponding to three spots, each of which was analyzed from 10 serial sections. (A) Absolute disaccharide ion abundances; (B) relative disaccharides ion abundances; ***, p value< 0.01, high significance; **, 0.01 < p value < 0.05, medium significance.

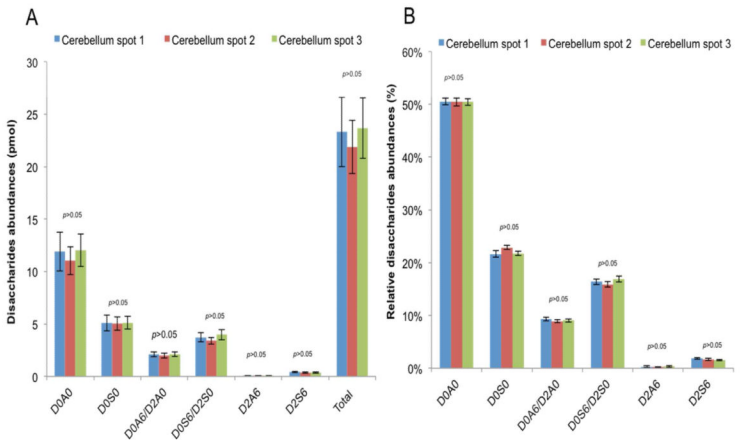

Figure 4.

Ion abundances of HS disaccharides from bovine brain cortex tissue slides corresponding to three spots, each of which was analyzed from 10 serial sections. (A) Absolute disaccharides ion abundances; (B) relative disaccharides ion abundances***, p value< 0.01, high significance; **, 0.01 < p value < 0.05, medium significance.

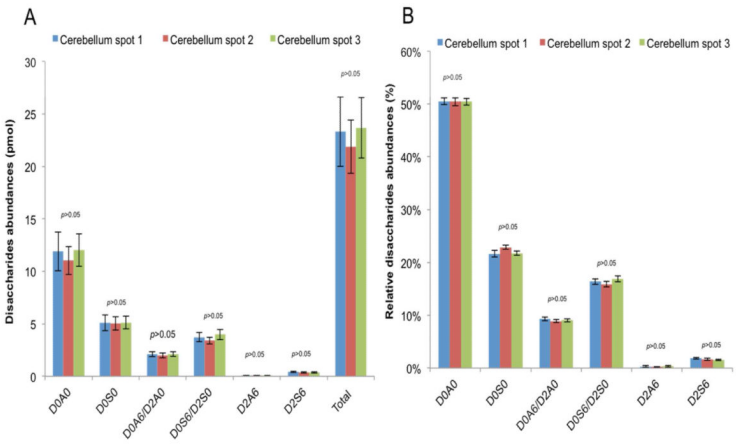

Figure 5.

Ion abundances of HS disaccharides from bovine brain cerebellum tissue slides corresponding to three spots, each of which was analyzed from 10 serial sections. (A) Absolute disaccharides ion abundances; (B) relative disaccharides ion abundances of disaccharides; ***, p value< 0.01, high significance; **, 0.01 < p value < 0.05, medium significance.

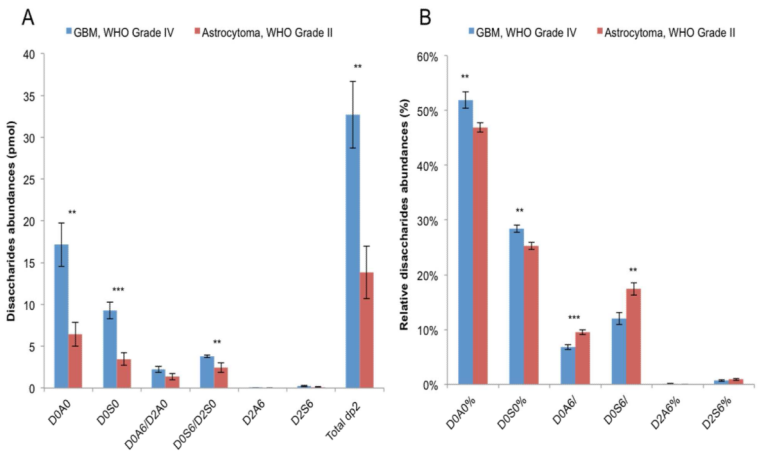

Figure 6.

The ion abundances of HS disaccharides released from human glioma slides. A set of three serial slides was used for the analysis of each individual. Astrocytoma (WHO grade II) samples from 3 individuals and GBM (WHO grade IV) samples from 4 individuals were obtained from biopsies. The mean value obtained from the set of individuals is shown. (A) Absolute disaccharides ion abundances; (B) relative disaccharides ion abundances. T-tests with two tailing were used for these data; ***, p value< 0.01, high significance; **, 0.01 < p value < 0.05, medium significance.